Role of CCL7 in Type I Hypersensitivity Reactions in Murine Experimental Allergic Conjunctivitis

Chuan-Hui Kuo,* Andrea M. Collins,* Douglas R. Boettner,* YanFen Yang,* and Santa J. Ono*,†,1

Molecules that are necessary for ocular hypersensitivity reactions include the receptors CCR1 and CCR3; CCL7 is a ligand for these receptors. Therefore, we explored the role of CCL7 in mast cell activity and motility in vitro and investigated the requirement for CCL7 in a murine model of IgE-mediated allergic conjunctivitis. For mast cells treated with IgE and Ag, the presence of CCL7 synergistically enhanced degranulation and calcium influx. CCL7 also induced chemotaxis in mast cells. CCL7-deficient bone marrow–derived mast cells showed decreased degranulation following IgE and Ag treatment compared with wild-type bone marrow–derived mast cells, but there was no difference in degranulation when cells were activated via an IgE-independent pathway. In vivo, CCL7 was upregulated in conjunctival tissue during an OVA-induced allergic response. Notably, the early-phase clinical symptoms in the conjunctiva after OVA challenge were significantly higher in OVA-sensitized wild-type mice than in control challenged wild-type mice; the increase was suppressed in CCL7-deficient mice. In the OVA-induced allergic response, the numbers of conjunctival mast cells were lower in CCL7-deficient mice than in wild-type mice. Our results demonstrate that CCL7 is required for maximal OVA-induced ocular anaphylaxis, mast cell recruitment in vivo, and maximal FcεRI-mediated mast cell activation in vitro. A better understanding of the role of CCL7 in mediating ocular hypersensitivity reactions will provide insights into mast cell function and novel treatments for allergic ocular diseases. ***The Journal of Immunology*****, 2017, 198: 645–656.**

Ocular allergies affect ∼20% of the United States population (1, 2). Mast cells, which originate in the bone marrow, play a critical role in allergic pathogenesis. In subsequent exposures following sensitization, cross-linking of allergen to IgE bound to FcεRI triggers signaling cascades that lead to activation of kinases, phosphatases, and GTPases. These enzymes induce degranulation and subsequently cause mast cells to release inflammatory mediators, including those already preformed in the cell (e.g., histamine, leukotrienes, and proteases) and others that are newly synthesized upon cell activation (e.g., cytokines, chemokines, and growth factors) (3, 4).

A growing body of evidence suggests that costimulatory molecules can enhance FcεRI-mediated mast cell activation. CC chemokines are key regulators of the early and late effector phases. Chemokines and their receptors are essential mediators in allergic reactions, because they control leukocyte migration and activity (5). Chemokines are highly expressed in a variety of allergic diseases, and polymorphisms in the genes encoding chemokines and their receptors may be risk factors for allergic diseases (6). Two CCLs, CCL3/MIP-1α and CCL11/eotaxin-1, appear to have critical roles in regulating mast cells in ocular allergy. These ligands bind to CCR1 and CCR3, respectively, exerting effects on the maturation and activation of mast cells (7, 8).

CCL11 does not induce mast cell degranulation (7, 9, 10), but it does promote mast cell differentiation (11). We reported that mice deficient for CCL11 or treated with a neutralizing Ab to this chemokine displayed reduced mast cell degranulation and impaired immediate hypersensitivity responses (12). Furthermore, mice deficient for CCR3 showed reductions in early-phase allergic symptoms, vascular leakage, and conjunctival eosinophil recruitment in a mouse model of allergic conjunctivitis (13–15).

In contrast to CCL11, CCL3 acts as a classical costimulatory factor, binding to CCR1 and enhancing FcεRI-mediated mast cell activation. CCL3 was reported to stimulate human mast cell degranulation in vitro (16) and murine mast cell degranulation in vitro and in vivo (7, 17). We found that treatment of mast cells with CCL3 and Ag results in greater degranulation than does cross-linking of FcεRI alone (8, 17). Mice in which CCL3 is deficient or neutralized fail to display typical allergic symptoms after ocular exposure to allergen. In other allergic diseases, mice deficient for CCR1 display reduced inflammatory responses (18–20), and treatment with a CCR1 antagonist reduced inflammation in a mouse model of allergic asthma (21). CCR1 is expressed by conjunctival mast cells, and subconjunctival injection of CCL3 increases conjunctival mast cell number and degranulation in vivo (7). The conjunctival mast cells in these mice displayed decreased degranulation compared with mast cells in wild-type mice (7).

*Division of Allergy and Immunology, Department of Pediatrics, Cincinnati Children's Hospital, Medical Center, Cincinnati, OH 45229; and †University of Cincinnati, Cincinnati, OH 45229

[1]Current address: Department of Ophthalmology & Visual Sciences, The University of British Columbia, Vancouver, BC, Canada.

ORCID: 0000-0002-0591-443X (D.R.B.).

Received for publication November 13, 2015. Accepted for publication November 15, 2016.

This work was supported by National Institutes of Health Grant R01-EY-019630/EY/NEI.

Address correspondence and reprint requests to Dr. Santa J. Ono at the current address: Office of the President, The University of British Columbia, 7th Floor, Walter C. Koerner Library, 1958 Main Mall, Vancouver, BC V6T 1Z2, Canada. E-mail address: sjo@ubc.ca

Abbreviations used in this article: BMMC, bone marrow–derived mast cell; CTMC, connective tissue mast cell; DNP-HSA, DNP–human serum albumin; EAC, experimental allergic conjunctivitis; m, mouse; RBL, rat basophilic leukemia; TRITC, tetramethylrhodamine.

Most analyses of FcεRI signaling focused on stimulation of the IgE receptor alone; the cellular events occurring in response to costimulation remain largely unexplored. We demonstrated previously that immediate cellular responses to costimulation of CCR1 and FcεRI include phosphorylation of p38 MAPK and production of the intermediate filament vimentin (22). We are particularly interested in the chemokines and cytokines produced in response to mast cell activation and identified genes that are upregulated in response to costimulation of FcεRI and CCR1 on mast cells. CCL7 was upregulated very strongly in our study (23). CCL7, previously known as monocyte-specific CCL3/MCP-3, belongs to the MCP subfamily of CCLs. CCL7 binds to CCR1, CCR2, and CCR3, is expressed at multiple sites of inflammation, and is produced by monocytes, fibroblasts, endothelial cells, and mast cells (24–26). Several studies suggest that CCL7 may be involved in vascular pathologies in which proliferation of smooth muscle cells plays an important role (27). CCL7 was shown to activate monocytes, basophils, and eosinophils, and it acts as a chemoattractant for a variety of cells, including those associated with allergy (e.g., monocytes, memory T lymphocytes, eosinophils, basophils, dendritic cells, and NK cells) (28–30). CCL7 was further linked to the pathology of a variety of allergic and inflammatory disease, including asthma (31, 32), airway inflammation in response to oxidative stress (33), aspirin allergy (34), and allergic rhinitis (35). CCL7 production is increased in mice that develop allergic lung inflammation in response to Arizona sand dust (36) and in mice challenged with respiratory allergens (37). CCL7 recruits neutrophils as part of airway inflammation in response to oxidative stress (33), and pretreatment of mice with anti-CCL7 reduces the inflammation and eosinophilia associated with respiratory allergy (37).

Although mast cells produce CCL7 and express receptors for CCL7, the role of this chemokine in regulating mast cell function is poorly characterized, and CCL7-deficient mice have yet to be used for studies of allergic diseases. In this study, we hypothesize that CCL7 is essential for maximal mast cell activation and recruitment and that CCL7 contributes to the development of allergic conjunctivitis symptoms in vivo. This hypothesis was tested using a rat basophilic leukemia (RBL)-2H3 cell line expressing CCR1 and bone marrow–derived murine mast cells that endogenously express CCRs, as well as by comparing symptoms of experimental conjunctivitis between wild-type and CCL7-deficienct mice.

Materials and Methods

Animals

$CCL7^{-/-}$ mice were obtained from the Jackson Laboratory (Bar Harbor, ME) and were maintained inbred on the C57BL/6J background. Age- and sex-matched wild-type animals were maintained under identical conditions. The present study conformed to all regulations for laboratory animal research outlined by the Animal Welfare Act, National Institutes of Health guidelines, and the Association for Research in Vision and Ophthalmology statement regarding the experimental use of animals and was approved by Cincinnati Children's Hospital Medical Center Committee on Animal Welfare.

Cell culture

RBL-CCR1 cells and RBL-2H3 cells (ATCC CRL-2256) (38) were maintained as monolayers in DMEM (+4500 mg/l glucose, +GlutaMAX, +pyruvate) supplemented with 15% FBS and 100 U/ml penicillin and streptomycin. The cells were maintained at 3.5×10^5 cells per milliliter and cultured at 37°C in 5% CO_2. Culture medium was refreshed every 3 d. Geneticin (G-418 sulfate, 1 mg/ml) was added to the medium of RBL-CCR1 cells, as described previously (8). To generate primary bone marrow–derived mast cells (BMMCs), low-density mononuclear cells were isolated from $CCL7^{-/-}$ and wild-type mice and cultured in RPMI 1640 medium containing 10% FBS, 2 mM glutamine, 100 U/ml penicillin, 10 μg/ml streptomycin, 0.1 mM nonessential amino acids, 50 μM 2-ME, and 10 mM HEPES in the presence of 20 ng/ml recombinant murine IL-3 and 10 ng/ml recombinant murine stem cell factor (both from PeproTech) for 4–6 wk (39). Tissue culture media and cell culture supplements were from Life Technologies, Invitrogen.

Cell phenotype was characterized by morphological examination after staining with toluidine blue or Giemsa stain (Diff-Quik) on Cytospin slides and by flow cytometry following staining with FITC-conjugated anti-FcεRI (eBioscience, San Diego, CA) and PE-conjugated anti–c-Kit (BioLegend). More than 90% of cultured cells were double positive for the mast cell markers FcεRI and c-Kit. Data were analyzed using FlowJo software (TreeStar, San Carlos, CA).

Induction and clinical evaluation of experimental allergic conjunctivitis

To induce experimental allergic conjunctivitis (EAC), mice were sensitized and challenged using an established protocol. In brief, mice were sensitized three times with 50 μg of OVA (grade V; Sigma-Aldrich) and 1 mg of aluminum hydroxide (Thermo Scientific) in 200 μl of sterile saline, using i.p. injections spaced 2 wk apart. Five weeks after the initial sensitization, a final challenge of 5 μl of saline, with or without 500 μg of OVA, was administered as eye drops. Control mice were mock sensitized in a similar manner using alum in saline and challenged using Ag solution. After the final challenge, four clinical responses were evaluated within the first 30 min and graded from 0 to 4, using defined criteria, by an ophthalmologist blinded to the treatment condition for each mouse (7). The cumulative clinical score was the sum of the scores for each of these four parameters (0–16).

Degranulation assay

RBL-CCR1 cells were cultured (4×10^4 cells per well) in DMEM culture media (Thermo Scientific) containing 10% FBS (Atlanta Biological), with or without 25 ng/ml anti–DNP IgE mAb (SPE7; Sigma-Aldrich), in a flat-bottom 96-well tissue culture plate overnight at 37°C. Subsequently, cells were washed twice with serum-free DMEM containing 0.1% BSA (Sigma-Aldrich) and stimulated or not for 20 min with 10 ng/ml DNP–human serum albumin (DNP-HSA; Sigma-Aldrich) and/or various concentrations of recombinant human CCL7 (R&D Systems) at 37°C. For BMMCs, 100 ng/ml DNP-IgE, recombinant mouse CCL7 (R&D systems), and Tyrode's solution were used. In some experiments, BMMCs were stimulated using different concentrations of calcium ionophore (0–10^4 nM; Sigma-Aldrich) for 20 min. After the stimulation, β-hexosaminidase activity in the supernatants was measured with 4-Nitrophenyl *N*-acetyl-β-D-glucosaminide (Sigma-Aldrich) in 0.1 M sodium citrate buffer (pH 4.5) for 60 min at 37°C. The reaction was stopped by the addition of 0.2 M glycine buffer (pH 10.5). The release of 4-p-nitrophenol was detected by absorbance at 405 nm. Total β-hexosaminidase activity was determined by lysing the cells in DMEM containing 0.1% Triton.

Calcium influx measurements

BMMCs were harvested and resuspended in standard culture medium, with or without 100 ng/ml IgE. After overnight culture at 37°C, the cells were harvested, washed with HEPES buffer, and incubated with 1 μM Fluo-4 AM (Molecular Probes), a calcium-sensitive fluorescent dye, for 60 min at 37°C. Cells were washed twice and suspended at 1×10^6 cells per milliliter in a calcium-free assay solution. Twenty-second measurements were collected prior to and immediately after the addition of 10 ng/ml DNP-HSA in the presence or absence of 10–100 ng/ml recombinant mouse CCL7. The subsequent release of internal stores of calcium was detected by assessing Fluo-4 fluorescence using a FACSCanto II flow cytometer (BD Biosciences, San Diego, CA) with excitation at 488 nm and emission at 520 nm. Data were analyzed using FlowJo software.

Chemotaxis assay

The assay was performed using 24-well Transwell cell culture chambers with 8.0 and 5.0 μm pore size (Corning Glass). RBL-CCR1 cells and BMMCs (1×10^6 cells/ml) were sensitized for 6 h with 25 and 100 ng/ml anti–DNP-IgE, respectively. After washing, the sensitized cells (2×10^4 cells in 100 μl of DMEM containing 0.5% BSA) were seeded in the upper compartment, and the lower compartment was filled with 500 μl of the same medium containing rCCL7. The chambers were incubated for 4 h at 37°C in 5% CO_2. The reaction was stopped by adding cold PBS containing 2% paraformaldehyde. The number of cells that passed through the membrane was quantified by staining with 0.4% trypan blue (Life Technologies, Invitrogen) and counting the number of cells present in at least four microscopic fields at 400× magnification.

ELISA

CCL7 and histamine were measured using a mouse MCP-3 Instant ELISA kit (eBioscience) and a histamine ELISA kit (Beckman Coulter), respectively. Total IgE, OVA-specific IgE, or OVA-specific IgG_1 in serum was measured using a Mouse IgE ELISA kit (eBioscience), an OVA-IgE ELISA kit (MD Bioproducts), or an OVA-IgG_1 ELISA kit (Alpha Diagnostic), respectively.

RNA extraction and quantitative real-time PCR

Total RNA was extracted using TRIzol Reagent (Invitrogen) and treated with DNase I (QIAGEN) before reverse transcription using the iScript cDNA Synthesis Kit (Bio-Rad), as per the manufacturer's instructions. Real-time RT-PCR was conducted using cDNA (20 ng), iQ SYBR Green Supermix (Bio-Rad), and the following individual primer sets: *Il6*, 5′-AATTCGGTACATCCTCGACGG-3′ (forward), 5′-GGTTGTTTTCTGCCAGTGCC-3′ (reverse); *Ccl7*, 5′-TGTCCTTTCTCAGAGTGGTTCT-3′ (forward), 5′-TGCTTCCATAGGGACATCATA-3′ (reverse); *Il4* (encoding IL-4), forward 5′-CTGTAGGGCTTCCAAGGTGCTTCG-3′, reverse 5′-CCATTTGCATGATGCTCTTTAGGC-3′; *Il13* (encoding IL-13), forward 5′-CATGGCGCTCTGGGTGACTG, reverse 5′-CGGCCAGGTCCACACTCCATAC-3′; and the housekeeping gene *Actb*, forward 5′-CGATGCCCTGAGGCTCTTTTCC-3′, reverse: 5′-CATCCTGTCAGCAATGCCTGGG-3′. Primers corresponding to *Ccl2*, *Ccl3*, *Ccl4*, and *Gapdh* were described previously (40). All primers were synthesized by MWG-Biotech. Fold changes were calculated after normalization to endogenous *Gapdh* using the comparative Ct method of relative quantification (41).

Western blotting

RBL-CCR1 cells and BMMCs were sensitized and then stimulated or not for 5 or 15 min with 10 ng/ml DNP-HSA (Sigma-Aldrich) and/or various concentrations of recombinant human CCL7 (R&D Systems) at 37°C. Total extracts of RBL-CCR1 cells were prepared in mammalian protein extraction reagent (M-PER and NE-PER; Pierce Chemical, Rockford, IL) containing protease inhibitors (cOmplete, Roche Diagnostic). BMMCs were prepared in RIPA lysis buffer containing protease and phosphatase inhibitors (ThermoFisher, Florence, KY). Protein concentrations were determined using a BCA Protein Assay Kit (Pierce). Equal amounts of RBL-CCR1 protein were separated using a 12% polyacrylamide SDS gel and transferred to a polyvinylidene fluoride membrane (both from Bio-Rad). After 1 h of blocking in 5% milk/TBS-Tween (0.1%), the membrane was incubated overnight at 4°C with rabbit polyclonal anti-β actin (ab8227; Abcam, Cambridge, MA), rabbit polyclonal anti–phospho-Akt (Ser^{473}), or rabbit polyclonal Akt (Cell Signaling Technology) Ab. Then the membrane was incubated with HRP-conjugated anti-rabbit IgG (Cell Signaling Technology). Protein expression was visualized using ECL chemiluminescent substrate (Pierce). Equal amounts of protein from BMMCs were separated using a 4–12% Bis-Tris Gel (NuPAGE Novex; Invitrogen) and transferred to a Nitrocellulose Pre-Cut Blotting Membrane (Invitrogen). After 1 h of blocking in Odyssey Blocking Buffer (TBS) (LI-COR), the membrane was incubated overnight at 4°C with rabbit polyclonal anti–β-actin (Abcam), rabbit polyclonal anti-phospho-Akt (Ser^{473}), or rabbit polyclonal Akt Ab (both from Cell Signaling Technology). Then the membrane was incubated with IRDye 800CW goat anti-rabbit secondary Abs (LI-COR). Protein expression was visualized using a scanner, and data were analyzed with Image Studio Lite software (both from LI-COR).

Flow cytometric analysis

Cells were blocked with unconjugated anti-FcγRII/III (2.4G2; BD Biosciences) and stained with FITC-conjugated anti-mouse FcεRIα (eBioscience), PE-conjugated anti-mouse CD117 (c-Kit) (BioLegend), FITC-conjugated anti-mouse CCR1 (BD Biosciences), or FITC- and PE-conjugated isotype-matched control Ig (eBioscience). Cells were analyzed using FACSDiva (BD Biosciences), and data were analyzed with FlowJo software.

Histological analyses

After sensitization and stimulation with rCCL7, RBL-CCR1 cells were fixed with 4% paraformaldehyde for 20 min. Then cells were washed with PBS and permeabilized with PBS containing 0.2% Triton X-100. After blocking with PBS containing 0.5% BSA, the cells were stained with 0.1 μg/ml tetramethylrhodamine (TRITC)-conjugated phalloidin (Sigma-Aldrich) for 30 min. Harvested eyes (including conjunctivas and eyelids) were fixed in 10% formaldehyde and embedded in paraffin, ensuring a cross-sectional orientation of all tissues. Sections (5 μm thick) were cut and stained metachromatically with 0.1% toluidine blue or naphthol AS-D chloroacetate esterase cytochemical. Mast cells in the lamina propria mucosae of the tarsal and bulbar conjunctivas were counted by blinded observers (42). The number of mast cells per square millimeter was determined using computer-generated image analysis (Image-Pro Plus; Media Cybernetics, Silver Spring, MD). For CCL7 detection in conjunctival tissue, ocular sections were stained with goat polyclonal anti–MCP-3 Ab (Santa Cruz Biotechnology) at 4°C overnight and then with Alexa Fluor 555–conjugated donkey anti-goat IgG (Invitrogen) for 1 h at room temperature. For detection of mast cell–inducing mouse (m)MCP-4 in conjunctival tissue, ocular sections were stained with goat polyclonal anti–mMCP-4 (MyBioSource) and anti-FcεRI at 4°C overnight and then with Alexa Fluor 555–conjugated donkey anti-goat IgG (Invitrogen) for 1 h at room temperature. Coverslips were mounted using Anti-Fade Dapi-Fluoromount-G (SouthernBiotech).

The extent of ruffling of each cell was scored by a researcher blinded to the treatment conditions using a scale of 0 to 2, with 0 = no ruffles present, 1 = ruffling confined to one area of the cell (no more than 25% of the cell's circumference), and 2 = two or more discrete areas of the cell contain ruffles. One hundred cells were assessed for each condition in three separate experiments.

Statistics

All analyses were performed with Prism 6.0 software (GraphPad, San Diego, CA). Statistical significance comparing two experimental groups was determined using the Student *t* test. When comparing multiple experimental groups, statistical differences were analyzed with one-way nonparametric ANOVA and ANOVA; $p < 0.05$ was considered statistically significant. Data are expressed as mean ± SEM, unless otherwise stated.

Results

CCL-7 and Ag synergistically induce degranulation in RBL-CCR1 cells and mouse BMMCs

Because CCL7 is a ligand for CCR1, we examined whether CCL7 could stimulate CCR1 and contribute to mast cell activation in a manner similar to that observed for another ligand, CCL3 (8). RBL-CCR1 cells and BMMCs derived from wild-type mice, which both display characteristics of mucosal-type mast cells, express CCR1; RBL-CCR1 cells express CCR1 but no other CCRs, whereas BMMCs cultured with stem cell factor express CCR1–5 (43). As shown in Fig. 1, degranulation of both cell types was significantly higher in the presence of Ag compared with the absence of Ag (RBL-CCR1, 28.4 ± 0.8 versus 8.1 ± 2.4%; BMMCs, 17.1 ± 0.5 versus 2.5 ± 0.02%; $p < 0.01$ for both). Significant enhancement of degranulation was observed with the addition of CCL7 to Ag–cross-linked RBL-CCR1 cells and BMMCs, starting at 10 ng/ml

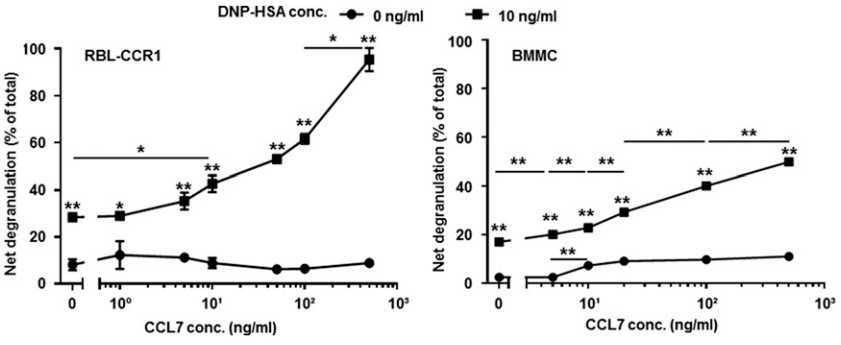

FIGURE 1. CCL-7 synergistically induces degranulation in RBL-CCR1 cells and mouse BMMCs. RBL-CCR1 cells and BMMCs were cultured or not with 25 or 100 ng/ml anti-DNP IgE for 16 h and then stimulated for 20 min with or without 10 ng/ml DNP-HSA and six concentrations of recombinant human or mouse CCL7. β-hexosaminidase activity was measured. Data are mean ± SEM and are representative of four separate experiments. $*p < 0.05$, $**p < 0.01$, ANOVA.

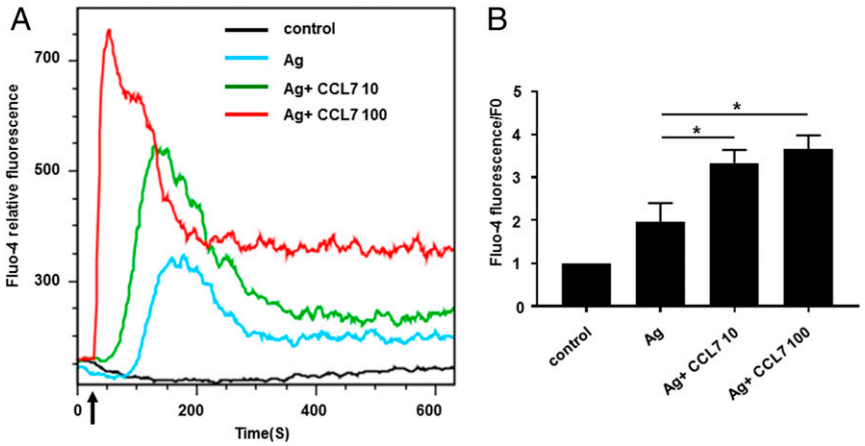

FIGURE 2. CCL-7 synergistically induces a significant increase in calcium influx in mouse BMMCs. Studies were performed with cultured BMMCs loaded with Fluo-4 AM. Fluorescence was measured over time before and after treatment with DNP-HSA with and without recombinant mouse CCL7. (**A**) Intracellular Ca^{2+} transient release and dose-response curves to CCL7. The arrow indicates the time of addition of DNP-has, with or without CCL7. The graph represents the average fluorescence intensity from cultured BMMCs. (**B**) The Fluo-4 ratio represents mean fluorescence after treatment (20–300 s)/mean baseline fluorescence before treatment (0–20 s). Data are mean ± SEM. The data shown are the average of the Fluo-4 ratio of four separate experiments. These studies were performed in the absence of extracellular calcium. *$p < 0.05$ from four experiments.

for RBL-CCR1 cells and at 0.1 ng/ml for BMMCs (Fig. 1). CCL7 induced a dose-dependent increase in the degranulation of RBL-CCR1 cells and BMMCs in the presence of Ag but not when Ag was absent in RBL-CCR1 cells (Fig. 1). A similar pattern was observed for calcium influx. A rise in intracellular calcium was observed from 0 s to 10 min for BMMCs (Fig. 2A), and the cells displayed a significant increase in calcium influx when costimulated with Ag and CCL7 compared with Ag alone (Fluo-4 fluorescence/F0 ratio: 2.0 ± 0.4 versus 3.3 ± 0.3 or 3.7 ± 0.3, $p < 0.05$; Fig. 2B). A similar degree of influx was observed for RBL-CCR1 cells (data not shown). Therefore, CCL7 might contribute to mast cell activation through cross-talk between the CCR1-mediated signaling pathway and the IgE receptor–mediated signaling pathway.

CCL7 induces chemotaxis of RBL-CCR1 cells and mouse BMMCs

CCL7 significantly and dose-dependently induced chemotaxis in both cell types. More than twice as many cells migrated across the

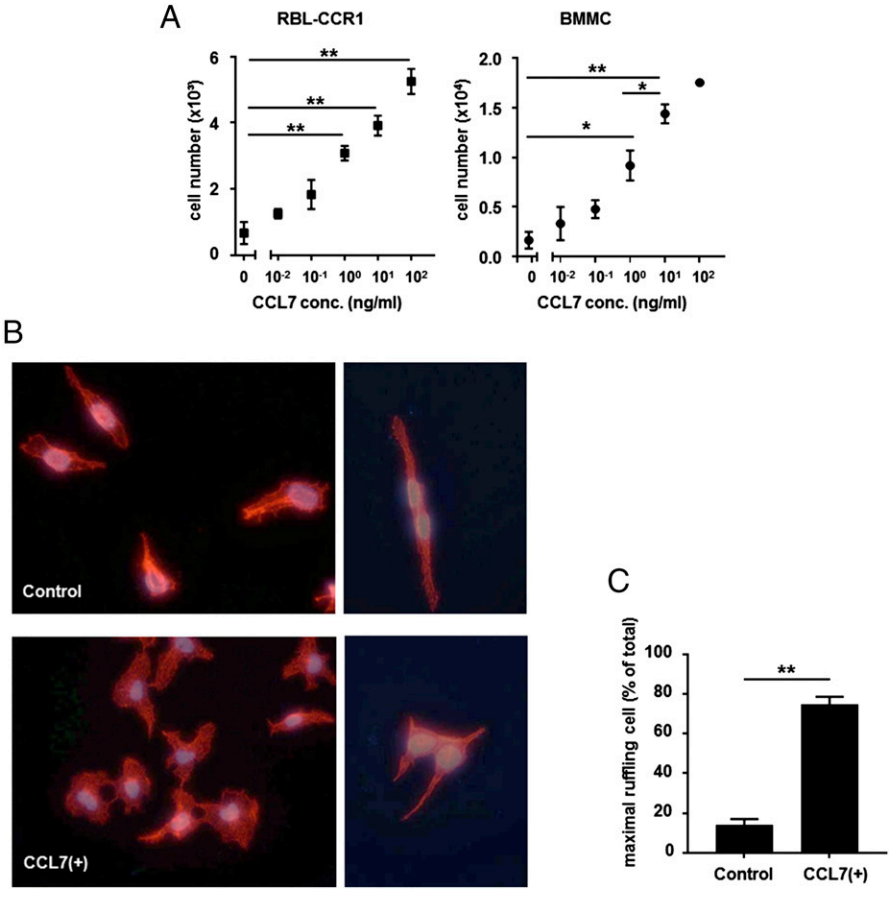

FIGURE 3. CCL7 induces chemotaxis of RBL-CCR1 cells and mouse BMMCs. (**A**) After sensitization with anti-DNP IgE, 2×10^4 RBL-CCR1 cells and BMMCs in serum-free medium were transferred to the upper compartment of a Transwell chamber; the lower compartment was filled with serum-free medium containing one of six concentrations (0–100 ng/ml) of recombinant human or mouse CCL7. Cells were incubated for 3 h before quantifying the number of migrated cells. (**B**) After sensitization with anti-DNP IgE, RBL-CCR1 cells were stimulated with 1 ng/ml recombinant human CCL7 or were left unstimulated. Then cells were fixed and processed for polymerized actin staining with TRITC-conjugated phalloidin. Original magnification ×40. (**C**) Ruffling for individual cells stimulated with control or CCL7 was assessed. For each group, 100 cells were counted per condition in three separate experiments. Data are mean ± SEM. *$p < 0.05$, **$p < 0.01$, ANOVA.

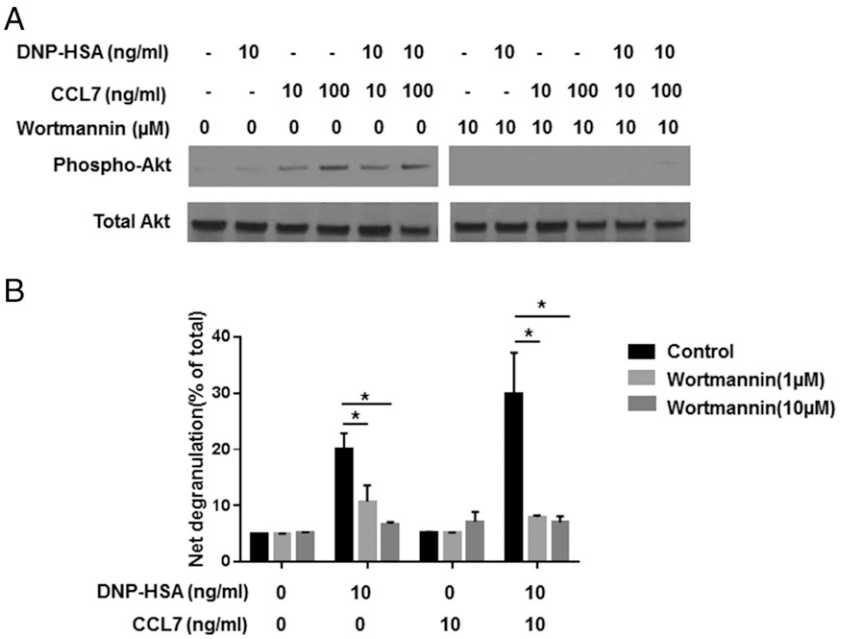

FIGURE 4. The Akt inhibitor wortmannin inhibits synergistic induction of degranulation by CCL7. (**A**) After sensitization, RBL-CCR1 cells were treated with wortmannin (10 μM) for 1 h before stimulation with CCL7 (10 and 100 ng/ml), with or without Ag (10 ng/ml), for 15 min. Cells were lysed, and Western blotting was performed using Abs against total Akt and phospho-Akt (Ser^{473}). Data are from one representative of two separate experiments. (**B**) After sensitization, BMMCs were treated with wortmannin (1 or 10 μM) or left untreated and then stimulated or not for 20 min with 10 ng/ml DNP-HSA and/or recombinant mouse CCL7. β-hexosaminidase activity was measured as a reflection of degranulation. Data are mean ± SEM and are representative of three separate experiments. *$p < 0.05$, ANOVA.

membrane in response to CCL7, even at 1 ng/ml; for 100 ng/ml, a ≥7-fold increase was observed (Fig. 3A). Rearrangement of the actin cytoskeleton is a crucial component of chemotaxis (44, 45). When actin changes in RBL-CCR1 cells were monitored by staining with TRITC-labeled phalloidin, dramatic membrane ruffling was observed within 60 s for CCL7-treated cells compared with control-treated cells (Fig. 3B). The extent of ruffling for each cell was scored, and the result showed that a higher proportion of cells displayed maximal membrane ruffling with CCL7 treatment compared with control (14 ± 3.06 versus 74.67 ± 4.98%, $p < 0.01$; Fig. 3C). The results indicate that CCL7 acts as a chemoattractant for mast cells in vitro.

CCL7 synergistically induces activation of the Akt pathway in RBL-CCR1 cells

Numerous chemoattractants trigger activation of PI3K in leukocytes. PI3K activation results in phosphorylation and activation of Akt/protein kinase B, a molecule that transmits signals that stimulate cell movement (46). Cross-linking of FcεRI in mouse mast cells also induces phosphorylation and enzymatic activation

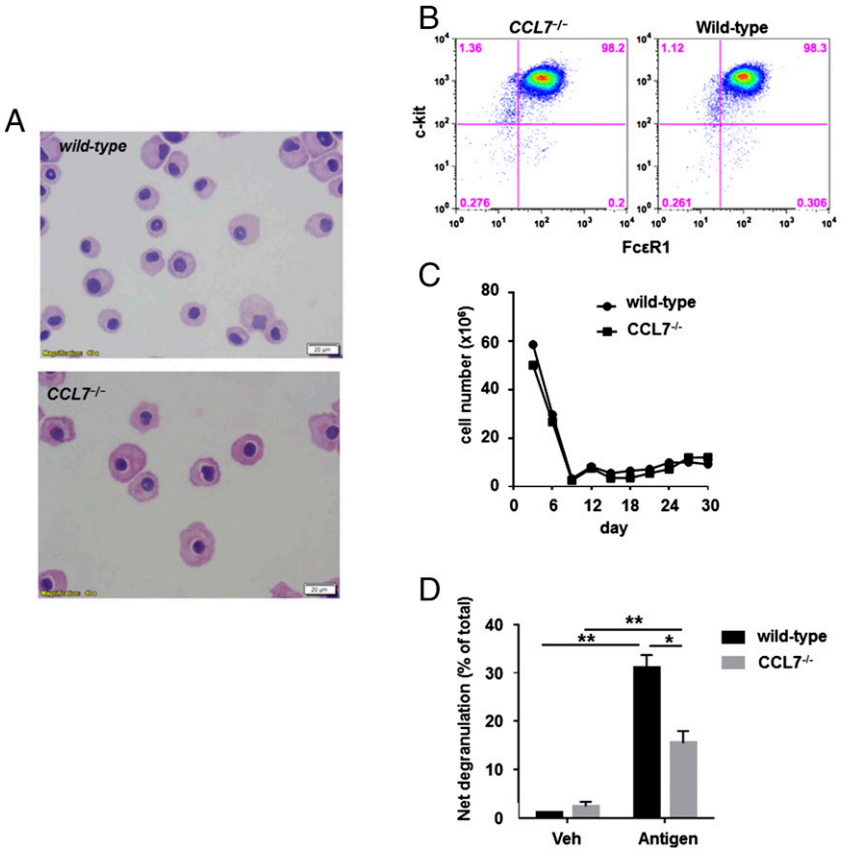

FIGURE 5. BMMCs cultured from $CCL7^{-/-}$ mice have no obvious defects in morphology, surface markers for mast cells, or proliferation, yet they display reduced degranulation in response to Ag stimulation. (**A**) Mature BMMCs (>4 wk of culture) from wild-type and $CCL7^{-/-}$ mice were stained with Giemsa to visualize morphology. Original magnification ×40. (**B**) Surface expression of FcεRI and c-kit on $CCL7^{-/-}$ BMMCs cultured for 5 wk was detected by flow cytometry. (**C**) Cell number was determined by staining with 0.4% trypan blue and counting cells using a hemocytometer. (**D**) BMMCs from wild-type and $CCL7^{-/-}$ mice were cultured with 100 ng/ml anti-DNP IgE for 16 h and then stimulated or not with 10 ng/ml DNP-HSA for 20 min. *$p < 0.05$, **$p < 0.01$, ANOVA.

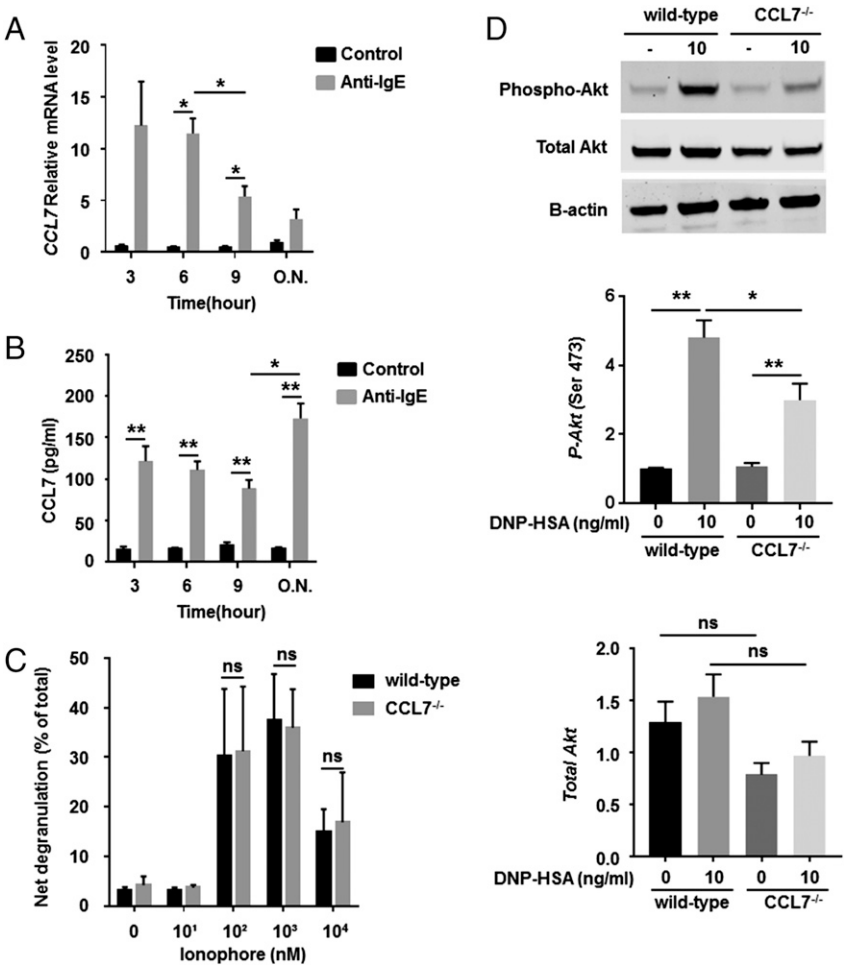

FIGURE 6. CCL7 is induced during anti-IgE sensitization, and its absence reduces Ag-induced Akt phosphorylation. Mature BMMCs (>4 wk of culture) from wild-type mice were sensitized or not with anti-DNP IgE (100 ng/ml), and levels of CCL7 mRNA and protein were quantified at different time points. (**A**) Total RNA from sensitized cells was isolated, and *Ccl7* expression was examined using real-time PCR. (**B**) Supernatants of culture medium were collected, and protein levels were analyzed by ELISA. (**C**) BMMCs were stimulated or not with different concentrations of ionophore for 20 min, and β-hexosaminidase activity was determined as a measure of degranulation. Data are mean ± SEM and are representative of four separate experiments. (**D**) A total of 1×10^6 BMMCs from wild-type and CCL7$^{-/-}$ mice was incubated overnight in medium containing anti-DNP IgE (100 ng/ml) and treated with 10 ng/ml Ag for 5 min. To examine the phosphorylation of Akt, Western blotting was performed on 30 μg of total protein using Abs to total Akt, phospho-Akt (Ser^{473}), and β-actin (loading control). Relative densitometric analysis is presented. Data are mean ± SEM and are representative of three separate experiments. *$p < 0.05$, **$p < 0.01$, ANOVA. ns, not significant.

of Akt, and PI3K-mediated Akt signaling is necessary for FcεRI-mediated degranulation (47, 48). To determine whether PI3K signaling pathways contribute to CCL7-induced mast cell activation, cells were treated with the PI3K/Akt inhibitor wortmannin for 1 h prior to treatment with CCL7. The PI3K/AKT inhibitor reduced levels of p-AKT associated with CCL7 treatment (Fig. 4A) and completely abrogated degranulation of RBL-CCR1 cells treated with DNP-HSA alone or with DNP-HSA and CCL7 (20.1 ± 2.8 versus 6.8 ± 0.3% and 29.9 ± 7.3 versus 7.1 ± 1.1%, respectively; $p < 0.05$ for both; Fig. 4B). The data suggest that the activation of mast cells by CCL7 is through PI3K/Akt pathways.

CCL7-deficient BMMCs show impaired degranulation in response to IgE–Ag stimulation

The potentiation of Ag-mediated degranulation may occur via autocrine secretion of G protein–coupled receptor ligands, such as CCL7, resulting in activation of signaling pathways. To determine whether autocrine CCL7 is required for optimal activation and motility of mast cells, we generated BMMCs from CCL7$^{-/-}$ mice. CCL7$^{-/-}$ BMMCs and wild-type BMMCs displayed similar morphology, proliferation during maturation, and expression of the surface markers FcεRI and c-Kit (Fig. 5A, 5C). Therefore, CCL7 is unlikely to be involved in mast cell differentiation and maturation. In contrast, degranulation induced by IgE–Ag was significantly and dramatically reduced for CCL7$^{-/-}$ BMMCs compared with wild-type BMMCs (15.5 ± 2.4 versus 31.1 ± 2.6%, $p < 0.05$, Fig. 5D). To test possible autocrine secretion of CCL7 through IgE-mediated activation in mast cells, we further measured CCL7 release and expression during sensitization. CCL7 transcription was induced under sensitization (Fig. 6A). CCL7 was also released continuously from 3 h to overnight by mast cells under IgE sensitization compared with untreated cells (Fig. 6B) (3 h: 121.6 ± 18.21 versus 16.06 ± 2.56 pg/ml; 6 h: 111.2 ± 10 versus 7.04 ± 0.43 pg/ml; 9 h: 88.9 ± 10.19 versus 21.43 ± 2.43 pg/ml; overnight: 173.3 ± 17.84 versus 17.04 ± 0.99 pg/ml, $p < 0.05$). To determine whether this is IgE–FcεRI pathway dependent, we also induced mast cell degranulation using calcium ionophore; there was no difference between CCL7$^{-/-}$ BMMCs and wild-type BMMCs (30.13 ± 3.52 versus 31.2 ± 3.36%, $p = 0.83$, Fig. 6C). To determine whether Akt activity is affected by CCL7 deficiency, its phosphorylation status was further studied in CCL7$^{-/-}$ BMMCs and wild-type BMMCs after IgE sensitization and Ag cross-linking. Western blot analysis showed that phosphorylation of Akt was reduced upon cross-linking of the IgE receptor, whereas total Akt levels remained constant (4.79 ± 0.50 versus 2.99 ± 0.48%, $p < 0.05$, Fig. 6D). Taken together, autocrine CCL7 production is critical for optimal IgE-mediated activation of mast cells through PI3K/Akt pathways.

CCL7 is upregulated during early-phase allergic responses in an in vivo model of allergic conjunctivitis

To further examine the role of CCL7 in situ, we examined its function in a model of EAC. In this model, an allergic reaction is induced in mice by systemically immunizing with OVA and then applying allergen locally via eye drops to the conjunctiva (Fig. 7A). A 6-fold increase in the expression of conjunctival *Ccl7* transcripts was observed within 30 min of local allergen exposure ($p < 0.05$ versus challenge with saline, Fig. 7B). Protein levels of

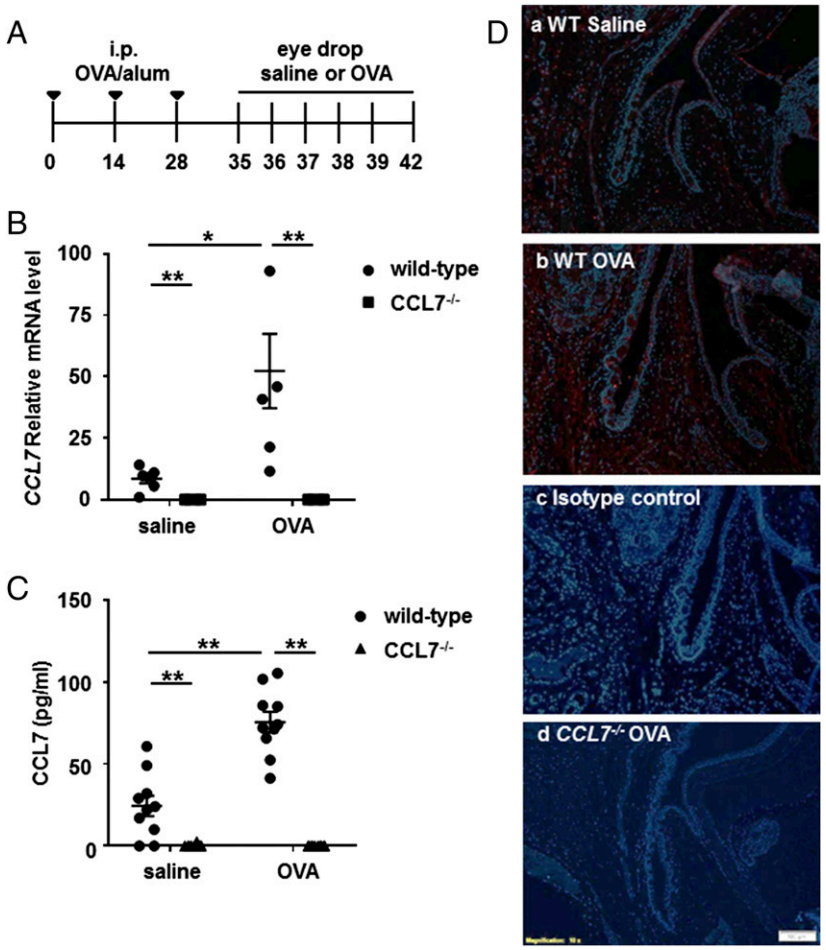

FIGURE 7. CCL7 is upregulated during the early-phase responses of EAC. (**A**) Time course for development of EAC. Mice were immunized i.p. with OVA and alum every other week for a total of three times, rested for 7 d, and repeatedly challenged with eye-drop administration of OVA or saline every day for a total of six times. (**B**) Total RNA from samples of conjunctival tissue was isolated 30 min after final challenge, and *Ccl7* expression levels were examined using real-time PCR. (**C**) Serum of mice was collected for ELISA analysis at 3 h after the final challenge. Data are mean ± SEM for $n = 5$ (B) and $n = 10$ (C) per group and are representative of four separate experiments. (**D**) Conjunctival tissues were fixed, serially sectioned, and stained for CCL7 using a polyclonal Ab. Localization of CCL7 (red) in the allergen-challenged conjunctiva of wild-type mice (**b**), saline (control)-challenged conjunctiva of wild-type mice (**a**), allergen-challenged conjunctiva of wild-type mice stained using the isotype-control Ab (**c**), and allergen-challenged conjunctiva of CCL7$^{-/-}$ mice (**d**) was examined using immunofluorescence. Original magnification ×10. Blue, DAPI. *$p < 0.05$, **$p < 0.01$, ANOVA.

CCL7 in the serum of OVA-challenged mice were also increased significantly compared with saline challenge (75.5 ± 6.3 versus 24.4 ± 6.2 pg/ml, $p < 0.01$, Fig. 7C). The CCL7 is likely produced by early-phase effector cells, because production of CCL7 by activated mast cells was reported (23). Neither CCL7 mRNA in the conjunctiva nor CCL7 protein in the serum was detected in CCL7-deficient mice (Fig. 7B, 7C). Histological analysis of CCL7 protein in ocular tissue showed widespread expression in OVA-challenged conjunctivas of wild-type mice, with the strongest intensity in the connective tissue, compared with ocular tissues from saline-challenged or CCL7-deficient mice (Fig. 7D).

CCL7$^{-/-}$ mice display markedly reduced clinical symptoms of ocular allergy

To evaluate the role of CCL7 in mast cell function in vivo, we compared acute-phase symptoms of ocular allergy in CCL7$^{-/-}$ and wild-type mice. Clinical symptoms of ocular allergy were scored within 30 min of ocular challenge with OVA. Acute clinical symptoms of immediate hypersensitivity, known to be mediated by mast cells, were significantly suppressed in CCL7$^{-/-}$ mice (Fig. 8A). Indeed, every symptom of clinical disease (i.e., conjunctival edema, lid edema, redness, tearing, and squinting) was reduced, albeit by differing degrees (data not shown). CCL7 clearly contributes to optimal mast cell activity in vivo. The low levels of histamine detected in the serum of CCL7$^{-/-}$ mice were similar to those in the serum of wild-type mice (Fig. 8B), indicating the local nature of the allergic response. The inductive phase of immune responses involves several biological pathways. Prior to secretion of allergen-specific IgE, Ag processing and presentation, B cell maturation, and class switching driven by Th2 cells must occur. Therefore, we examined the synthesis of Igs in CCL7$^{-/-}$ mice challenged with OVA. OVA challenge resulted in significantly higher levels of total IgE, OVA-specific IgE, and OVA-specific IgG_1 (all indicative of Th2 responses) in the serum of wild-type and CCL7$^{-/-}$ mice (Fig. 8C–E). Surprisingly, total IgE and OVA-specific IgE concentrations were significantly lower in the serum of OVA-challenged CCL7$^{-/-}$ mice compared with wild-type mice ($p < 0.001$), whereas OVA-IgG_1 levels were comparable for the two mouse strains (Fig. 8E). Therefore, the effects of CCL7 on Th2-driven Ab production are restricted to the generation of IgE Abs.

Mast cell recruitment following allergen challenge is reduced in CCL7$^{-/-}$ mice

To determine whether the mast cell chemotaxis response observed in vitro is reflected in the in vivo mouse model of ocular allergy, the number of mast cells in the ocular tissue of wild-type and CCL7$^{-/-}$ mice exposed to OVA was determined. A reduction in the number of conjunctival mast cells was observed with toluidine blue staining (33.4 ± 6.3 to 15.7 ± 2.6 per square millimeter, $p < 0.01$, Fig. 9A) and with chloroacetate esterase staining (Fig. 9B). No statistically significant difference in the number of conjunctival mast cells was observed between wild-type and CCL7$^{-/-}$ mice for saline-challenged eyes (11.14 ± 2.4 versus 11.57 ± 1.6 per square millimeter, $p = 0.34$, Fig. 9A).

Mast cell activation induces degranulation and release of inflammatory mediators, including histamine, cytokines, proteoglycans, and proteases. Mast cell expression of neutral proteases (mMCP-4, mMCP-5, mMCP-6, and carboxypeptidase A) is typically ascribed to the connective tissue mast cell (CTMC) subset

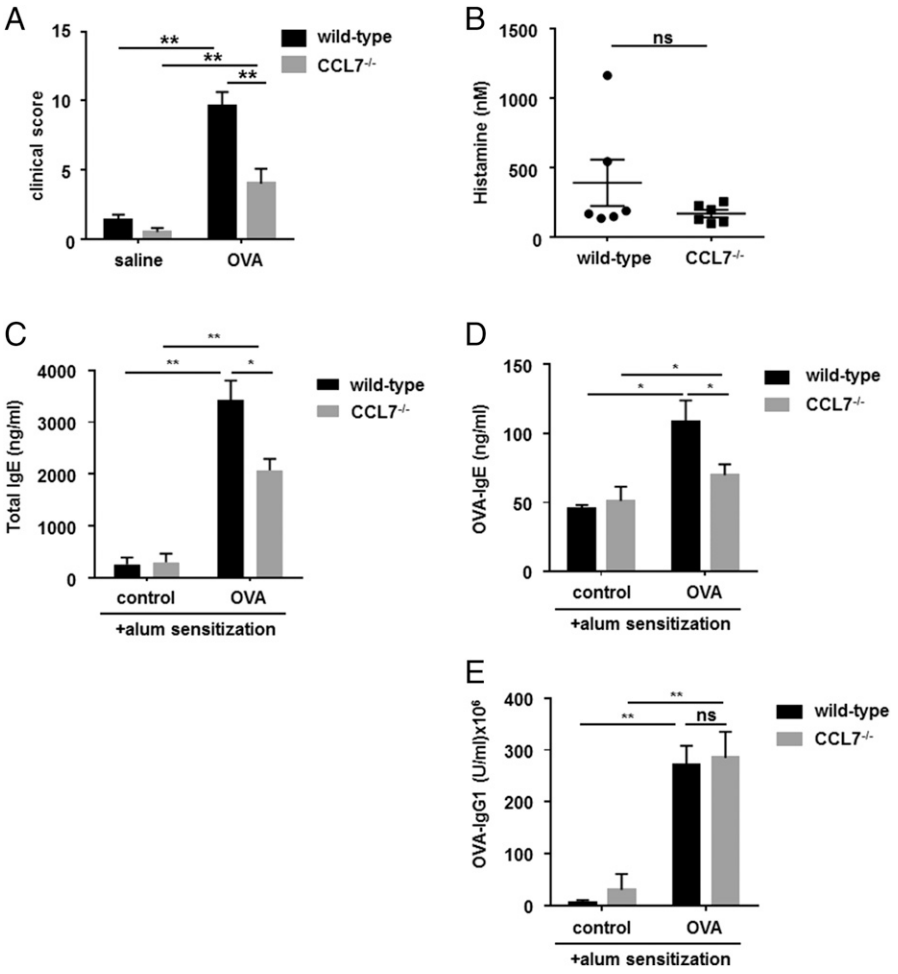

FIGURE 8. CCL7$^{-/-}$ mice have impaired allergen-induced immediate hypersensitivity reactions. Levels of IgE Abs, but not IgG_1 Abs, are reduced in the serum of CCL7$^{-/-}$ mice with experimental allergen-induced conjunctivitis. (**A**) Wild-type control mice and CCL7$^{-/-}$ mice were sensitized and challenged with OVA or saline control. The allergen-induced clinical symptoms (clinical scores, taking into account conjunctival edema, lid edema, redness, tearing, and squinting) were analyzed 15 min after the final challenge as parameters of immediate hypersensitivity. (**B**) Histamine levels in the serum of the mice, obtained 3 h after the final challenge, were analyzed by ELISA. The data are representative of four separate experiments. Levels of total IgE (**C**), OVA-specific IgE (**D**), and IgG_1 (**E**) in the serum of saline-challenged (control) or OVA-challenged wild-type and CCL7$^{-/-}$ mice were determined by ELISA. Data are mean ± SEM and are representative of four separate experiments (n = 6 per group). *$p < 0.05$, **$p < 0.01$, ANOVA. ns, not significant.

(49). To further characterize local mast cells in the allergic conjunctiva, we performed immunofluorescence staining to identify mMCP-4–containing mast cells. A significant reduction in the number of mMCP-4$^+$ mast cells was observed in the conjunctival samples from CCL7$^{-/-}$ mice compared with wild-type mice when exposed to OVA (8.83 ± 1.85 versus 21.22 ± 1.77 per square millimeter, $p < 0.005$, Fig. 10). No statistically significant difference in the number of mMCP-4$^+$ mast cells was observed between wild-type mice and CCL7$^{-/-}$ mice challenged with saline (4.57 ± 1.56 versus 7.5 ± 2.5 per square millimeter, $p = 0.61$,

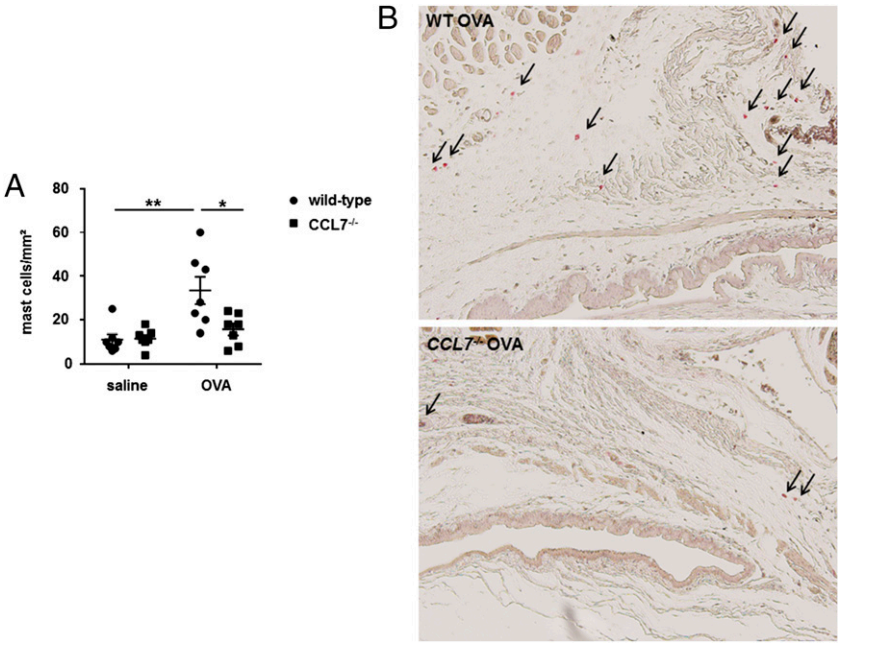

FIGURE 9. CCL7$^{-/-}$ mice display reduced mast cell recruitment in allergen-induced conjunctivitis. Conjunctival tissue of wild-type control mice and CCL7$^{-/-}$ mice sensitized and challenged with OVA and saline was harvested, fixed, serially sectioned, and stained for mast cells using toluidine blue or chloroacetate esterase staining. (**A**) Total mast cell number was counted in toluidine blue–stained conjunctival tissue 3 h after final Ag or control challenge. (**B**) Chloroacetate esterase–stained conjunctival tissue from OVA-sensitized wild-type and CCL7$^{-/-}$ mice was examined to detect the localization of mast cells (red) (arrows) 3 h after the final Ag challenge. Original magnification ×10. Data are mean ± SEM and are representative of four separate experiments (n = 7 per group). *$p < 0.05$, Student t test.

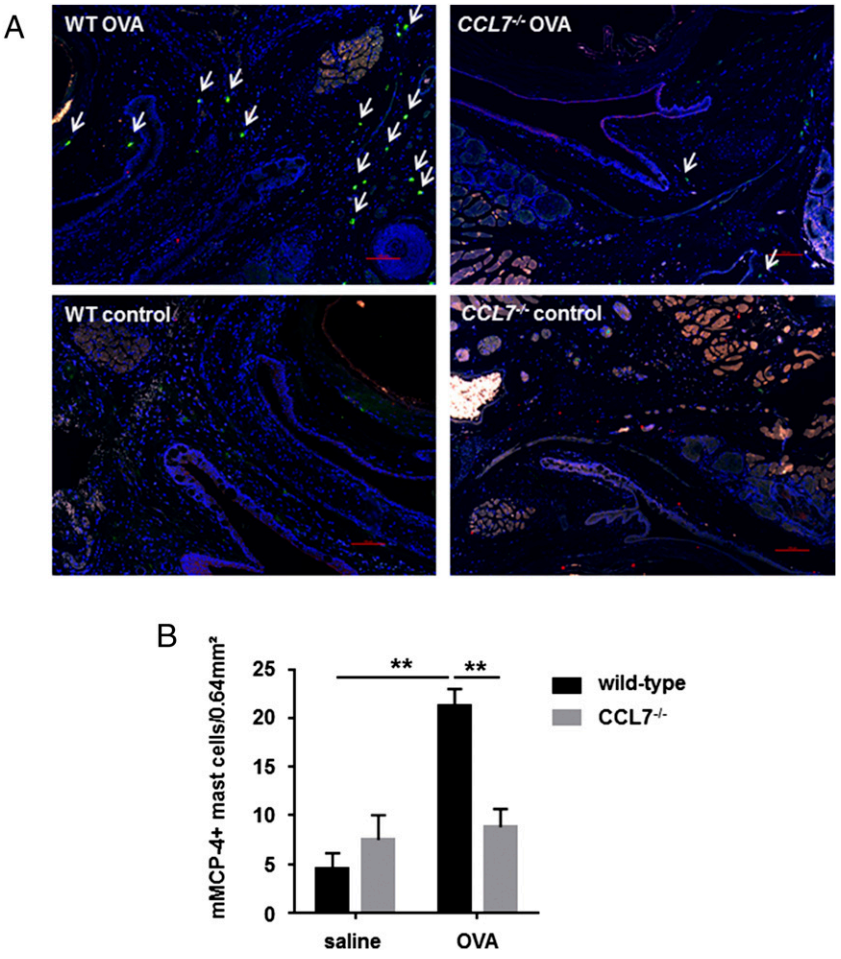

FIGURE 10. CCL7$^{-/-}$ mice display reduced numbers of mMCP-4^{+} mast cells during allergen-induced conjunctivitis. Conjunctival tissues of wild-type control mice and CCL7$^{-/-}$ mice, sensitized and challenged with OVA or saline, were harvested, fixed, serially sectioned, and stained for mMCP-4, c-kit, and FcεRI. (**A**) Conjunctival tissue was examined to detect the localization of mMCP-4^{+} mast cells (green immunofluorescence) (arrows) 3 h after the final challenge with Ag or control in OVA-sensitized wild-type and CCL7$^{-/-}$ mice. Original magnification ×20, Blue, DAPI. (**B**) mMCP-4^{+} mast cell number was counted in conjunctival tissues 3 h after the final challenge. Data are mean ± SEM and are representative of four separate experiments ($n > 5$ per group). $^{**}p < 0.01$, ANOVA.

Fig. 10B). Taken together, these data suggest that CCL7 contributes to recruitment of mast cells to the conjunctiva in mice experiencing allergic hypersensitivity reactions.

CCL7$^{-/-}$ mice display reduced levels of chemokines and cytokines in allergen-induced conjunctivitis

Various chemokines and cytokines are synthesized upon activation of mast cells via cross-linking of FcεRI (40, 50). To examine whether the absence of CCL7 affects the production of inflammatory mediators in allergic conjunctivitis, mRNA expression of representative CCLs and cytokines was measured using real-time PCR. In wild-type mice, expression of the chemokines *Ccl2, Ccl3*, and *Ccl4* and the cytokines *Il4*, *Il6*, and *Il13* increased following OVA challenge compared with control challenge in OVA-sensitized mice (Fig. 11). For CC7$^{-/-}$ mice challenged with OVA, expression levels of *Ccl2*, *Ccl3*, *Ccl4*, and *Il4* were reduced significantly compared with wild-type mice; levels of *Il6* and *Il13* were comparable (Fig. 11). No significant differences in expression were observed between control-challenged CCL7$^{-/-}$ and wild-type mice. These data suggest that CCL7 deficiency reduces the production of chemokines and cytokines and might, by this mechanism, limit mast cell recruitment and possible mast cell activation in allergic conjunctivitis.

Discussion

Development of better therapies for immunological disorders, such as allergy, will require identification of mediators of IgE-dependent mast cell activation. To our knowledge, this study is the first report of CCL7's contributions to mast cell function in allergen-induced conjunctivitis. CCL7-mediated enhancement of mast cell activation was observed for RBL-CCR1 cells, which express only one CCL7 receptor, and for BMMCs, which express all three CCL7 receptors (CCR1, CCR2, and CCR3); this suggests that CCL7 acts via CCR1 to enhance Ag-mediated mast cell activation. We further demonstrated that CCL7 acts as a mast cell chemoattractant, as well as an inducer of mast cell activation, and that CCL7-mediated phosphorylation of Akt likely contributes to degranulation. Akt is one of the major players of the signaling cascade; it can be activated by G protein–coupled receptors that induce production of phosphatidylinositol (3,4,5)-trisphosphates by PI3K (48). Phosphorylation of Akt at Ser^{473} stimulates full enzymatic activity. In this study, CCL7 increased Akt phosphorylation in mast cells, and wortmannin, a specific inhibitor of PI3K, significantly attenuated Akt phosphorylation and degranulation of mast cells in the presence of Ag and CCL7. Previously, we found that CCL3 synergistically enhances FcεRI-mediated expression of cytokines and chemokines (e.g., CCL2, CCL7, TNF-α, and IL-6) by mast cells. CCL7 is strongly upregulated in mast cells that are stimulated by FcεRI cross-linking alone and, to a greater extent, by costimulation of FcεRI and CCR1 (1, 23), which suggests autocrine contributions of CCL7 to mast cell function. Cultured CCL7$^{-/-}$ BMMCs expressed surface markers of mast cells, and there was no proliferation difference during maturation between wild-type and CCL7$^{-/-}$ BMMCs; therefore, CCL7 might not be critical for mast cell differentiation. However, the induction of CCL7 during mast cell sensitization and the decreased degranulation observed for mast cells lacking CCL7 suggest that autocrine CCL7 is essential for mast cell activation. The reduction in Akt phosphorylation observed in Ag–cross-linked mast cells lacking CCL7 suggests a role for autocrine CCL7 in mast cell function

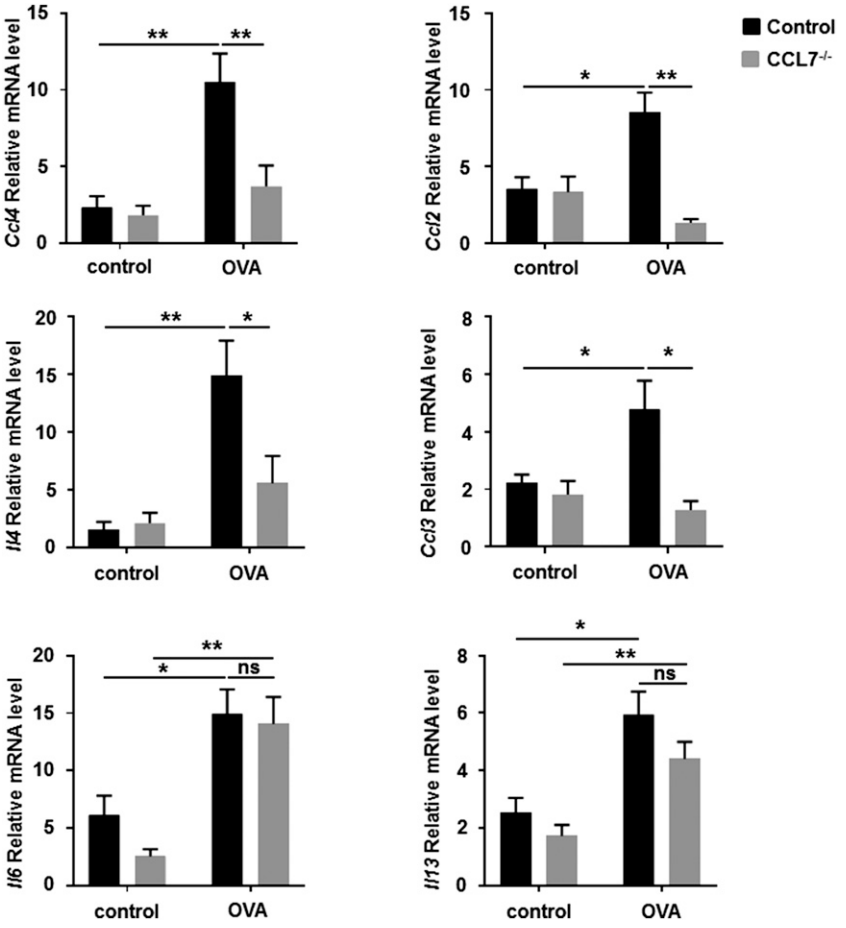

FIGURE 11. CCL7$^{-/-}$ mice display reduced expression of chemokines and cytokines in allergen-induced conjunctivitis. Wild-type and CCL7$^{-/-}$ mice were challenged with Ag or saline. Total mRNA from conjunctival tissue was isolated 30 min after the final challenge, and mRNA expression levels for *Ccl2*, *Ccl3*, *Ccl4*, *Il4*, *Il6*, and *Il13* were examined using real-time PCR. Data are mean ± SEM and are representative of four separate experiments (n = 5 per group). *$p < 0.05$, **$p < 0.01$, ANOVA. ns, not significant.

through activation of the PI3K/Akt pathway. Other investigators reported that CCL7 alone did not stimulate degranulation (51) or migration (52) of HMC-1 human mast cells or histamine release by mouse peritoneal mast cells (53); however, our studies focus on CCL7 in the presence of Ag, and mast cells from different tissues are known to have different responses (54).

The reductions in allergic symptoms and mast cell recruitment observed for CCL7-deficient mice provide a particularly compelling argument for the importance of this chemokine in promoting acute hypersensitivity reactions. The importance of CCL7 is further supported by the increase in its production observed in wild-type mice exposed to ocular allergens. Serine proteinases with trypsin-like (tryptase) and chymotrypsin-like (chymase) properties are major constituents of mast cell granules. Humans express only one mast cell chymase, whereas mature murine mast cells express mMCP-1, mMCP-2, mMCP-4, and/or mMCP-5, depending on tissue location, substrate specificity, and affinity for proteoglycans. Mast cell expression of neutral proteases typically ascribed to the mucosal mast cell subset (mMCP-1 and mMCP-2) or the CTMC subset (mMCP-4, mMCP-5, mMCP-6, and carboxypeptidase) was examined (49). We reported previously that mast cells in the murine conjunctiva are CTMCs (55), a finding that was confirmed in this study by immunostaining for mMCP-4. Expression of mMCP-4 was reduced, as was expression of chemokines and cytokines, in the allergic conjunctiva of CCL7-deficient mice. This implies that CCL7 plays a critical role in the functions of mast cells in vivo. Other investigators reported that CCL7 produced by B cells facilitated the mobilization of monocytes from bone marrow and triggered monocyte migration into injured heart tissue (56). We found that mature and undifferentiated BMMCs were attracted to rCCL7 (data not shown), suggesting that CCL7 might recruit mast cell progenitors from bone marrow to allergic tissues.

CCL7 was reported to be an important molecular effector of host resistance to infection. CCL7 recruits IL-4$^+$ Th2 leukocytes to the site of *Leishmania* infection and cooperates with CCL2 to regulate IL-4 production during intracellular infection (57). CCL7 directly regulates IL-4 through engagement of CCR2 on dendritic cells. CCR2-deficient bone marrow–derived dendritic cells produce IL-4 and stimulate production of IL-4 by T cells (58). It is interesting that CCL7 deficiency affected Ag sensitization (i.e., production of allergen-specific IgE Abs) in our model of allergic conjunctivitis. During allergic responses, activated mast cells and other cells produce the Th2 cytokines IL-4 and IL-13, which bind to receptors containing IL-4Rα on a variety of cells, including T cells, B cells, monocytes, endothelial cells, epithelial cells, and fibroblasts. Upon binding of IL-4 or IL-13 to IL-4Rα, STAT6 is phosphorylated. STAT6 function is critical for allergy, because STAT6-deficient mice have impaired Th2 function and B cell class switching to IgE (59). Numerous IL-4 and IL-13 gene variants were associated with elevated IgE levels and atopic conditions, including ocular allergy (6, 60). We also observed reduction of *Il4* expression in CCL7$^{-/-}$ mice with EAC. CCL7$^{-/-}$ mice might have a defect in STAT6 activation or function, which would result in decreased levels of allergen-specific IgE. This, in turn, would manifest in depressed mast cell degranulation upon challenge, because the level of mast cell receptor for Ag would be affected. However, FcεRI expression is comparable in the conjunctiva of untreated CCL7$^{-/-}$ and wild-type mice (data not shown), and there was no difference in the level of OVA-IgG$_1$ in CCL7$^{-/-}$ mice compared with wild-type mice; therefore, the impaired mast

cell activation may not entirely relate to levels of Ig. CCL7 deficiency could decrease mast cell activation and clinical symptoms in a direct or indirect manner. *Ccl2*, *Ccl3*, and *Ccl4* were all reduced in CCL7$^{-/-}$ mice with EAC. These chemokines are potent mediators of chemotaxis for basophils, eosinophils, and mononuclear cells (61, 62). They are also involved in the activation of eosinophils and basophils during allergic inflammation (63). CCL2 is produced by a wide variety of cells, including mast cells (43), and a role for the CCL2/CCR2 axis in recruiting mast cell progenitors was reported in the context of pulmonary inflammation (64). The reduction in expression of other CCLs as a result of CCL7 deficiency supports a possible role for CCL7 in mast cell activation and motility.

Mast cell activity may be increased in an autocrine fashion by activating or secreting chemicals during the early-phase allergic response or even at the sensitization phase, and factors secreted by mast cells can influence other cell types that contribute to allergic responses, particularly during the late phase. Future work should address the potential involvement of CCL7 in late-phase reactions, because CCL7 was reported to affect motility and activity of eosinophils (28, 30).

In conclusion, we demonstrated that CCL7 plays roles in mast cell motility and maximal FcεRI-mediated mast cell activation in vitro and is essential for the development of maximal acute responses in allergen-induced conjunctivitis. The findings of these studies will have important implications for chemokine-targeting treatments of hypersensitivity responses.

Acknowledgments

We thank Anne Goodwin for editorial assistance. We also thank Dr. Marc Rothenberg and his laboratory, especially Melissa Mingler, for valuable assistance.

Disclosures

The authors have no financial conflicts of interest.

References

1. Saban, D. R., V. Calder, C. H. Kuo, N. J. Reyes, D. A. Dartt, S. J. Ono, and J. Y. Niederkorn. 2013. New twists to an old story: novel concepts in the pathogenesis of allergic eye disease. *Curr. Eye Res.* 38: 317–330.
2. O'Brien, T. P. 2013. Allergic conjunctivitis: an update on diagnosis and management. *Curr. Opin. Allergy Clin. Immunol.* 13: 543–549.
3. Gilfillan, A. M., and C. Tkaczyk. 2006. Integrated signalling pathways for mast-cell activation. *Nat. Rev. Immunol.* 6: 218–230.
4. Galli, S. J., and M. Tsai. 2008. Mast cells: versatile regulators of inflammation, tissue remodeling, host defense and homeostasis. *J. Dermatol. Sci.* 49: 7–19.
5. Toda, M., T. Nakamura, M. Ohbayashi, Y. Ikeda, M. Dawson, C. C. Aye, D. Miyazaki, and S. J. Ono. 2007. Mechanisms of leukocyte trafficking in allergic diseases: insights into new therapies targeting chemokines and chemokine receptors. *Expert Rev. Clin. Immunol.* 3: 351–364.
6. Toda, M., and S. J. Ono. 2002. Genomics and proteomics of allergic disease. *Immunology* 106: 1–10.
7. Miyazaki, D., T. Nakamura, M. Toda, K. W. Cheung-Chau, R. M. Richardson, and S. J. Ono. 2005. Macrophage inflammatory protein-1α as a costimulatory signal for mast cell-mediated immediate hypersensitivity reactions. *J. Clin. Invest.* 115: 434–442.
8. Toda, M., M. Dawson, T. Nakamura, P. M. Munro, R. M. Richardson, M. Bailly, and S. J. Ono. 2004. Impact of engagement of FcepsilonRI and CC chemokine receptor 1 on mast cell activation and motility. *J. Biol. Chem.* 279: 48443–48448.
9. Romagnani, P., A. De Paulis, C. Beltrame, F. Annunziato, V. Dente, E. Maggi, S. Romagnani, and G. Marone. 1999. Tryptase-chymase double-positive human mast cells express the eotaxin receptor CCR3 and are attracted by CCR3-binding chemokines. *Am. J. Pathol.* 155: 1195–1204.
10. Ochi, H., W. M. Hirani, Q. Yuan, D. S. Friend, K. F. Austen, and J. A. Boyce. 1999. T helper cell type 2 cytokine-mediated comitogenic responses and CCR3 expression during differentiation of human mast cells in vitro. *J. Exp. Med.* 190: 267–280.
11. Quackenbush, E. J., B. K. Wershil, V. Aguirre, and J. C. Gutierrez-Ramos. 1998. Eotaxin modulates myelopoiesis and mast cell development from embryonic hematopoietic progenitors. *Blood* 92: 1887–1897.
12. Miyazaki, D., T. Nakamura, M. Ohbayashi, C. H. Kuo, N. Komatsu, K. Yakura, T. Tominaga, Y. Inoue, H. Higashi, M. Murata, et al. 2009. Ablation of type I hypersensitivity in experimental allergic conjunctivitis by eotaxin-1/CCR3 blockade. *Int. Immunol.* 21: 187–201.
13. Fukuda, K., C. H. Kuo, K. Morohoshi, F. T. Liu, and S. J. Ono. 2012. The murine CCR3 receptor regulates both eosinophilia and hyperresponsiveness in IgE-mediated allergic conjunctivitis. *Br. J. Ophthalmol.* 96: 1132–1136.
14. Nakamura, T., M. Ohbayashi, M. Toda, D. A. Hall, C. M. Horgan, and S. J. Ono. 2005. A specific CCR3 chemokine receptor antagonist inhibits both early and late phase allergic inflammation in the conjunctiva. *Immunol. Res.* 33: 213–221.
15. Komatsu, N., D. Miyazaki, T. Tominaga, C. H. Kuo, S. Namba, S. Takeda, H. Higashi, and Y. Inoue. 2008. Transcriptional analyses before and after suppression of immediate hypersensitivity reactions by CCR3 blockade in eyes with experimental allergic conjunctivitis. *Invest. Ophthalmol. Vis. Sci.* 49: 5307–5313.
16. Alam, R., P. A. Forsythe, S. Stafford, M. A. Lett-Brown, and J. A. Grant. 1992. Macrophage inflammatory protein-1 α activates basophils and mast cells. *J. Exp. Med.* 176: 781–786.
17. Fifadara, N. H., C. C. Aye, S. K. Raghuwanshi, R. M. Richardson, and S. J. Ono. 2009. CCR1 expression and signal transduction by murine BMMC results in secretion of TNF-α, TGFbeta-1 and IL-6. *Int. Immunol.* 21: 991–1001.
18. Liehn, E. A., M. W. Merx, O. Postea, S. Becher, Y. D. Talab, E. Shagdarsuren, M. Kelm, A. Zernecke, and C. Weber. 2007. Ccr1 deficiency reduces inflammatory remodelling and preserves left ventricular function after myocardial infarction. *J. Cell. Mol. Med* 12: 496–506.
19. Amat, M., C. F. Benjamim, L. M. Williams, N. Prats, E. Terricabras, J. Beleta, S. L. Kunkel, and N. Godessart. 2006. Pharmacological blockade of CCR1 ameliorates murine arthritis and alters cytokine networks in vivo. *Br. J. Pharmacol.* 149: 666–675.
20. Chou, R. C., N. D. Kim, C. D. Sadik, E. Seung, Y. Lan, M. H. Byrne, B. Haribabu, Y. Iwakura, and A. D. Luster. 2010. Lipid-cytokine-chemokine cascade drives neutrophil recruitment in a murine model of inflammatory arthritis. *Immunity* 33: 266–278.
21. Carpenter, K. J., J. L. Ewing, J. M. Schuh, T. L. Ness, S. L. Kunkel, M. Aparici, M. Miralpeix, and C. M. Hogaboam. 2005. Therapeutic targeting of CCR1 attenuates established chronic fungal asthma in mice. *Br. J. Pharmacol.* 145: 1160–1172.
22. Toda, M., C. H. Kuo, S. K. Borman, R. M. Richardson, A. Inoko, M. Inagaki, A. Collins, K. Schneider, and S. J. Ono. 2012. Evidence that formation of vimentin mitogen-activated protein kinase (MAPK) complex mediates mast cell activation following FcεRI/CC chemokine receptor 1 cross-talk. *J. Biol. Chem.* 287: 24516–24524.
23. Aye, C. C., M. Toda, K. Morohoshi, and S. J. Ono. 2012. Identification of genes and proteins specifically regulated by costimulation of mast cell Fcε receptor I and chemokine receptor 1. *Exp. Mol. Pathol.* 92: 267–274.
24. Jacobsson, B., R. M. Holst, B. Andersson, and H. Hagberg. 2005. Monocyte chemotactic protein-2 and -3 in amniotic fluid: relationship to microbial invasion of the amniotic cavity, intra-amniotic inflammation and preterm delivery. *Acta Obstet. Gynecol. Scand.* 84: 566–571.
25. Schenk, S., N. Mal, A. Finan, M. Zhang, M. Kiedrowski, Z. Popovic, P. M. McCarthy, and M. S. Penn. 2007. Monocyte chemotactic protein-3 is a myocardial mesenchymal stem cell homing factor. *Stem Cells* 25: 245–251.
26. Wakahara, S., Y. Fujii, T. Nakao, K. Tsuritani, T. Hara, H. Saito, and C. Ra. 2001. Gene expression profiles for Fc ε RI, cytokines and chemokines upon Fc ε RI activation in human cultured mast cells derived from peripheral blood. *Cytokine* 16: 143–152.
27. Maddaluno, M., M. Di Lauro, A. Di Pascale, R. Santamaria, A. Guglielmotti, G. Grassia, and A. Ialenti. 2011. Monocyte chemotactic protein-3 induces human coronary smooth muscle cell proliferation. *Atherosclerosis* 217: 113–119.
28. Dahinden, C. A., T. Geiser, T. Brunner, V. von Tscharner, D. Caput, P. Ferrara, A. Minty, and M. Baggiolini. 1994. Monocyte chemotactic protein 3 is a most effective basophil- and eosinophil-activating chemokine. *J. Exp. Med.* 179: 751–756.
29. Xu, L. L., D. W. McVicar, A. Ben-Baruch, D. B. Kuhns, J. Johnston, J. J. Oppenheim, and J. M. Wang. 1995. Monocyte chemotactic protein-3 (MCP3) interacts with multiple leukocyte receptors: binding and signaling of MCP3 through shared as well as unique receptors on monocytes and neutrophils. *Eur. J. Immunol.* 25: 2612–2617.
30. Fujisawa, T., Y. Kato, H. Nagase, J. Atsuta, A. Terada, K. Iguchi, H. Kamiya, Y. Morita, M. Kitaura, H. Kawasaki, et al. 2000. Chemokines induce eosinophil degranulation through CCR-3. *J. Allergy Clin. Immunol.* 106: 507–513.
31. Batra, J., S. Das, R. Chatterjee, S. Chandra, and B. Ghosh. 2011. Monocyte chemotactic protein (MCP3) promoter polymorphism is associated with atopic asthma in the Indian population. *J. Allergy Clin. Immunol.* 128: 239–242.e233.
32. Rojas-Ramos, E., A. F. Avalos, L. Pérez-Fernandez, F. Cuevas-Schacht, E. Valencia-Maqueda, and L. M. Terán. 2003. Role of the chemokines RANTES, monocyte chemotactic proteins-3 and -4, and eotaxins-1 and -2 in childhood asthma. *Eur. Respir. J.* 22: 310–316.
33. Michalec, L., B. K. Choudhury, E. Postlethwait, J. S. Wild, R. Alam, M. Lett-Brown, and S. Sur. 2002. CCL7 and CXCL10 orchestrate oxidative stress-induced neutrophilic lung inflammation. *J. Immunol.* 168: 846–852.
34. Kupczyk, M., Z. Kurmanowska, I. Kupryś-Lipińska, M. Bocheńska-Marciniak, and P. Kuna. 2010. Mediators of inflammation in nasal lavage from aspirin intolerant patients after aspirin challenge. *Respir. Med.* 104: 1404–1409.
35. Christodoulopoulos, P., E. Wright, S. Frenkiel, A. Luster, and Q. Hamid. 1999. Monocyte chemotactic proteins in allergen-induced inflammation in the nasal mucosa: effect of topical corticosteroids. *J. Allergy Clin. Immunol.* 103: 1036–1044.
36. Ichinose, T., S. Yoshida, K. Sadakane, H. Takano, R. Yanagisawa, K. Inoue, M. Nishikawa, I. Mori, H. Kawazato, A. Yasuda, and T. Shibamoto. 2008. Effects of Asian sand dust, Arizona sand dust, amorphous silica and aluminum oxide on allergic inflammation in the murine lung. *Inhal. Toxicol.* 20: 685–694.

37. Stafford, S., H. Li, P. A. Forsythe, M. Ryan, R. Bravo, and R. Alam. 1997. Monocyte chemotactic protein-3 (MCP-3)/fibroblast-induced cytokine (FIC) in eosinophilic inflammation of the airways and the inhibitory effects of an anti-MCP-3/FIC antibody. *J. Immunol.* 158: 4953–4960.
38. Richardson, R. M., B. C. Pridgen, B. Haribabu, and R. Snyderman. 2000. Regulation of the human chemokine receptor CCR1. Cross-regulation by CXCR1 and CXCR2. *J. Biol. Chem.* 275: 9201–9208.
39. Groschwitz, K. R., R. Ahrens, H. Osterfeld, M. F. Gurish, X. Han, M. Abrink, F. D. Finkelman, G. Pejler, and S. P. Hogan. 2009. Mast cells regulate homeostatic intestinal epithelial migration and barrier function by a chymase/Mcpt4-dependent mechanism. *Proc. Natl. Acad. Sci. USA* 106: 22381–22386.
40. Yamada, N., H. Matsushima, Y. Tagaya, S. Shimada, and S. I. Katz. 2003. Generation of a large number of connective tissue type mast cells by culture of murine fetal skin cells. *J. Invest. Dermatol.* 121: 1425–1432.
41. Pfaffl, M. W. 2001. A new mathematical model for relative quantification in real-time RT-PCR. *Nucleic Acids Res.* 29: e45.
42. Ishida, W., E. Tsuru, A. Tominaga, J. I. Miyazaki, T. Higuchi, S. Sakamoto, and A. Fukushima. 2009. Systemic overexpression of IFN-gamma and IL-5 exacerbates early phase reaction and conjunctival eosinophilia, respectively, in experimental allergic conjunctivitis. *Br. J. Ophthalmol.* 93: 1680–1685.
43. Oliveira, S. H., and N. W. Lukacs. 2001. Stem cell factor and IgE-stimulated murine mast cells produce chemokines (CCL2, CCL17, CCL22) and express chemokine receptors. *Inflamm. Res.* 50: 168–174.
44. Hall, A. 1998. Rho GTPases and the actin cytoskeleton. *Science* 279: 509–514.
45. Ridley, A. J., M. A. Schwartz, K. Burridge, R. A. Firtel, M. H. Ginsberg, G. Borisy, J. T. Parsons, and A. R. Horwitz. 2003. Cell migration: integrating signals from front to back. *Science* 302: 1704–1709.
46. Artemenko, Y., T. J. Lampert, and P. N. Devreotes. 2014. Moving towards a paradigm: common mechanisms of chemotactic signaling in *Dictyostelium* and mammalian leukocytes. *Cell. Mol. Life Sci.* 71: 3711–3747.
47. Takayama, G., M. Ohtani, A. Minowa, S. Matsuda, and S. Koyasu. 2013. Class I PI3K-mediated Akt and ERK signals play a critical role in FcεRI-induced degranulation in mast cells. *Int. Immunol.* 25: 215–220.
48. Kitaura, J., K. Asai, M. Maeda-Yamamoto, Y. Kawakami, U. Kikkawa, and T. Kawakami. 2000. Akt-dependent cytokine production in mast cells. *J. Exp. Med.* 192: 729–740.
49. Welle, M. 1997. Development, significance, and heterogeneity of mast cells with particular regard to the mast cell-specific proteases chymase and tryptase. *J. Leukoc. Biol.* 61: 233–245.
50. Zhao, W., C. A. Oskeritzian, A. L. Pozez, and L. B. Schwartz. 2005. Cytokine production by skin-derived mast cells: endogenous proteases are responsible for degradation of cytokines. *J. Immunol.* 175: 2635–2642.
51. Hartmann, K., F. Beiglböck, B. M. Czarnetzki, and T. Zuberbier. 1995. Effect of CC chemokines on mediator release from human skin mast cells and basophils. *Int. Arch. Allergy Immunol.* 108: 224–230.
52. Hartmann, K., B. M. Henz, S. Krüger-Krasagakes, J. Köhl, R. Burger, S. Guhl, I. Haase, U. Lippert, and T. Zuberbier. 1997. C3a and C5a stimulate chemotaxis of human mast cells. *Blood* 89: 2863–2870.
53. Alam, R., P. Forsythe, S. Stafford, J. Heinrich, R. Bravo, P. Proost, and J. Van Damme. 1994. Monocyte chemotactic protein-2, monocyte chemotactic protein-3, and fibroblast-induced cytokine. Three new chemokines induce chemotaxis and activation of basophils. *J. Immunol.* 153: 3155–3159.
54. Forsythe, P., and M. Ennis. 2000. Clinical consequences of mast cell heterogeneity. *Inflamm. Res.* 49: 147–154.
55. Fukuda, K., M. Ohbayashi, K. Morohoshi, L. Zhang, F. T. Liu, and S. J. Ono. 2009. Critical role of IgE-dependent mast cell activation in a murine model of allergic conjunctivitis. *J. Allergy Clin. Immunol.* 124: 827–833.e2.
56. Zouggari, Y., H. Ait-Oufella, P. Bonnin, T. Simon, A. P. Sage, C. Guérin, J. Vilar, G. Caligiuri, D. Tsiantoulas, L. Laurans, et al. 2013. B lymphocytes trigger monocyte mobilization and impair heart function after acute myocardial infarction. *Nat. Med.* 19: 1273–1280.
57. Katzman, S. D., and D. J. Fowell. 2008. Pathogen-imposed skewing of mouse chemokine and cytokine expression at the infected tissue site. *J. Clin. Invest.* 118: 801–811.
58. Fiorina, P., M. Jurewicz, A. Vergani, A. Augello, J. Paez, V. Ricchiuti, V. Tchipachvili, M. H. Sayegh, and R. Abdi. 2008. Phenotypic and functional differences between wild-type and $CCR2^{-/-}$ dendritic cells: implications for islet transplantation. *Transplantation* 85: 1030–1038.
59. Geha, R. S., H. H. Jabara, and S. R. Brodeur. 2003. The regulation of immunoglobulin E class-switch recombination. *Nat. Rev. Immunol.* 3: 721–732.
60. Potaczek, D. P., and M. Kabesch. 2012. Current concepts of IgE regulation and impact of genetic determinants. *Clin. Exp. Allergy* 42: 852–871.
61. Borish, L. C., and J. W. Steinke. 2003. 2. Cytokines and chemokines. *J. Allergy Clin. Immunol.* 111(2 Suppl.): S460–S475.
62. Schall, T. J., K. Bacon, R. D. Camp, J. W. Kaspari, and D. V. Goeddel. 1993. Human macrophage inflammatory protein alpha (MIP-1 alpha) and MIP-1 beta chemokines attract distinct populations of lymphocytes. *J. Exp. Med.* 177: 1821–1826.
63. Kuna, P., S. R. Reddigari, T. J. Schall, D. Rucinski, M. Sadick, and A. P. Kaplan. 1993. Characterization of the human basophil response to cytokines, growth factors, and histamine releasing factors of the intercrine/chemokine family. *J. Immunol.* 150: 1932–1943.
64. Collington, S. J., J. Hallgren, J. E. Pease, T. G. Jones, B. J. Rollins, J. Westwick, K. F. Austen, T. J. Williams, M. F. Gurish, and C. L. Weller. 2010. The role of the CCL2/CCR2 axis in mouse mast cell migration in vitro and in vivo. *J. Immunol.* 184: 6114–6123.